Accurate calibration and control of relative humidity close to 100% by X-raying a DOPC multilayer

Yicong Ma[a], **Sajal K. Ghosh**[a,†], **Sambhunath Bera**[b,‡], **Zhang Jiang**[c], **Stephanie Tristram-Nagle**[d], **Laurence B. Lurio**[b], and **Sunil K. Sinha**[a]

Sunil K. Sinha: ssinha@physics.ucsd.edu

[a]Department of Physics, University of California-San Diego, La Jolla, CA-92093, USA

[b]Department of Physics, Northern Illinois University, DeKalb, IL-60115, USA

[c]Advanced Photon Source, Argonne National Laboratory, Argonne, IL-60439, USA

[d]Biological Physics Group, Department of Physics, Carnegie Mellon University, Pittsburgh, PA-15213, USA

Abstract

In this study, we have designed a compact sample chamber that can achieve accurate and continuous control of the relative humidity (RH) in the vicinity of 100%. A 1,2-dioleoyl-*sn-glycero*-3-phosphocholine (DOPC) multilayer can be used as a humidity sensor by measuring its inter-layer repeat distance (*d*-spacing) *via* X-ray diffraction. We convert from DOPC *d*-spacing to RH according to a theory given in the literature and previously measured data of DOPC multilamellar vesicles in polyvinylpyrrolidone (PVP) solutions. This curve can be used for calibration of RH close to 100%, a regime where conventional sensors do not have sufficient accuracy. We demonstrate that this control method can provide RH accuracies of 0.1 to 0.01%, which is a factor of 10–100 improvement compared to existing methods of humidity control. Our method provides fine tuning capability of RH continuously for a single sample, whereas the PVP solution method requires new samples to be made for each PVP concentration. The use of this cell also potentially removes the need for an X-ray or neutron beam to pass through bulk water if one wishes to work close to biologically relevant conditions of nearly 100% RH.

Introduction

There are currently two commonly used methods for relative humidity (RH) control. One utilizes air/water vapor flow, for which the accuracy is usually ±1 to 2% for the RH range from 0% to 95%. The second method involves placing a reservoir with saturated salt solution in the chamber, which gives a discrete number of values of the RH, depending on the kind of salt used, *e.g.*, NaCl for 75% RH and K_2SO_4 for 97% RH. Both methods require a uniform temperature environment. A small temperature fluctuation or a temperature

Correspondence to: Sunil K. Sinha, ssinha@physics.ucsd.edu.

[†]Current address: Department of Physics, Shiv Nadar University, Chithera, Dadri, Gautam Budh Nagar, UP 203207, India.
[‡]Current address: Department of Physics, University of California-San Diego, La Jolla, CA-92093, USA.

gradient would easily result in ±1% to ±2% error in RH. To our knowledge, accurate and continuous humidity control with an error of less than ±0.1% for high humidity values (95–100% RH) has not been shown with these methods. To achieve high accuracy humidity control close to 100% RH, one must control the temperature gradient and have an accurate measure of the RH. No existing RH sensor in the market can measure with accuracy close to or better than 0.1%. To design such accurate RH control, one needs to address both issues carefully.

Temperature uniformity and stability throughout the whole sample chamber is very difficult to control within such a small tolerance. This is exactly the cause of the widely debated "vapor pressure paradox" for lipid membranes,[1] where better than 99% RH was not achieved. It has been experimentally proved by Katsaras that once the temperature gradient is eliminated, 100% RH can be achieved and no paradox exists.[2,3] The Nagle group has also designed a chamber to achieve 100% RH for lipid bilayer X-ray measurements,[4,5] and neutron measurements (see www.humidity.frank-heinrich.net).

In order to achieve not only 100% RH, but also accurate and continuous control for a range of high relative humidities close to 100%, we have developed a chamber which controls a temperature differential. This method has been used previously for surface wetting studies.[6–8]

In order to obtain an accurate measurement of RH, we need to use a calibration sample that responds very sensitively to RH changes close to 100%. We have chosen to use the lamellar repeat spacing of a 1,2-dioleoyl-*sn-glycero*-3-phosphocholine (DOPC) multilayer as a calibrant. It is well known that the water uptake of lipids responds very sensitively when the RH gets close to 100%. Although the possibility of using a supported lipid multilayer to measure RH has been previously mentioned in the literature,[9] no rigorous calibration of the *d*-spacing *vs.* RH curve has been carried out directly with vapor chambers. This is mainly due to the lack of RH sensors with sufficient accuracy. In this study, we will try to establish this calibration standard by consolidating the theory given in the literature with the published data of DOPC multi-lamellar vesicles in polyvinylpyrrolidone (PVP) solution, and use this curve as the calibration curve for our data with supported DOPC multilayers in a vapor chamber.

Chamber design

There are two main parts in our chamber design: the reservoir and the sample. A reservoir consisting of a 1% (mole fraction) K_2SO_4 solution serves as the humidity source which generates a constant water vapor pressure (we call this relative humidity the reference RH). The sample is located where the desired RH is created. There are two independent temperature control loops: temperature control for the reservoir and temperature control for the sample. The two parts are connected *via* a weak thermal link. A schematic of the temperature control setup is given in Fig. 1.

By controlling the temperature of the reservoir, T_{res}, and the temperature of the sample, T_{sam}, we can control the temperature difference $T = T_{res} - T_{sam}$. The distribution of water molecules in the water vapor will re-arrange according to the temperature gradient, which

results in a re-distribution of relative humidity. As demonstrated in Fig. 2: when $T = 0$ the sample is at the reference RH for 1% K_2SO_4 solution. Note that the use of an unsaturated salt solution produces an approximately temperature independent RH. When $T < 0$, RH of the sample is lower than the reference RH (Fig. 2(c)); similarly when $T > 0$, it is higher (Fig. 2(a)).

Fig. 3 shows pictures of our humidity controlled sample chamber used as a cell for X-ray diffraction and optical microscopy measurements. The chamber consists of two parts: the top (Fig. 3(b)) with reservoir and the bottom (Fig. 3(c)) with sample. The two parts have independent temperature control loops, and are thermally separated by a Teflon© ring. The reservoir solution is contained in a sponge. The sponge and the sample are kept in close contact with the respective part of the sample chamber to favor temperature equilibration. The sample chamber is constructed with copper to ensure good thermal uniformity. A Lakeshore temperature controller with two control loops is used for the temperature control.

Calibration of the DOPC *d*-spacing *vs.* relative humidity curve

Measurements of a DOPC multilayer as a standard sample were carried out to measure the RH of the sample environment. X-ray diffraction measurements of the lamellar repeat distance or *d*-spacing of the DOPC multilayer sample are a sensitive measure of the RH of the sample environment, since the uptake of water between the bilayers depends sensitively on RH particularly as the RH tends to 100%. In our experiments, the sample temperature is kept constant at 31 °C while the reservoir temperature is raised to increase the RH at the sample. The DOPC multilayers are deposited using spreading method developed by Li *et al.*[10] and were annealed at 50 °C for 1–2 days in a humidity chamber after taking out from the vacuum.

The X-ray measurements were taken on the diffractometer at sector 33 BM at the Advanced Photon Source, Argonne National Laboratory with a 20 keV X-ray beam. Fig. 4 shows one set of diffraction measurements of a typical DOPC sample over a range of temperature gradient. The RH ranges from 97.1% to 100.000% if converted from measured *d*-spacing with the standard curve discussed below. As RH increases the diffraction peaks shift to lower q_z, which means the *d*-spacing is increasing. The gradual distortion and disappearance of higher orders of Bragg peaks is due to the increased undulations due to increased hydration, as explained by Nagle and Tristram-Nagle,[11–13] as well as by Salditt.[14]

There is no obvious standard established in the literature for converting from *d*-spacing to RH. The data which do exist contradict each other.[15,16] We have resolved this conflict by using a theoretical model combined with existing experimental measurements.

I. Derivation of osmotic pressure

In order to calibrate our data for *d*-spacing as a function of RH, we will compare our results with measurements of the *d*-spacing of DOPC multilammelar vesicles in solution, where the osmotic pressure of the solution has been modified by the addition of PVP, a high molecular weight polymer. These measurements should be comparable, since the osmotic pressure in solution, and the RH in vapor should have identical effects on the chemical potential of

water in the multilayers. According to Petrache *et al.*,[17] the osmotic pressure of the multilayer, P_{osm}, can be decomposed into three contributions, a Helfrich fluctuation pressure, P_{fl}, a hydration pressure, P_h, and a van der Waals pressure P_{vdW};

$$P_{osm} = P_{fl} + P_h + P_{vdw}. \quad (1)$$

The fluctuation pressure, P_{fl}, depends on the thickness of the water layer, a and can be approximated with an exponential function with a decay length λ_{fl} of the form,

$$P_{fl} = A_{fl} e^{-a/\lambda_{fl}}. \quad (2)$$

The hydration pressure, P_h can be written in a similar fashion in terms of a decay length λ_h,

$$P_h == A_h e^{-a/\lambda_h}. \quad (3)$$

The van der Waals pressure,[18] P_{vdW} has the form,

$$P_{vdw} = \frac{H}{6\pi} \left(-\frac{2}{(D'_B + a)^3} + \frac{1}{(2D'_B + a)^3} + \frac{1}{a^3} \right). \quad (4)$$

Here, H is a Hamaker constant, D_B' is the bilayer thickness and a the water thickness. $D_B' + a = d$, is the d-spacing of the multilayer.

In order to determine the values for the parameters A_{fl}, λ_{fl}, A_h, λ_h, H and D_B' for DOPC, we need to fit this expression for P_{osm} to the experimental data.

II. Fitting data from Hristova and White[16] and Tristram-Nagle *et al.*[11]

In the paper by Hristova and White published in 1998,[16] a list of d-spacings *vs.* RH from 34% to 93% and PVP weight fractions from nominal 60% to 5% is given, as well as the number of water molecules per lipid n_w. In order to get a calibration curve for RH > 95%, we took the 60% to 5% weight fraction PVP data and translated it into osmotic pressure.

To convert PVP concentration to osmotic pressure, we use the method described by Vink[19] in 1971. The concentration c can be calculated from the PVP weight fraction w,

$$c = \frac{w}{w v_2 + (1 - w) v_1}. \quad (5)$$

Osmotic pressure can then be calculated using the relation;

$$P = A_1 c + A_2 c^2 + A_3 c^3. \quad (6)$$

The values of υ_1, υ_2, A_1, A_2, A_3 are taken from the same paper.[19] The PVP weight fractions are taken with values that are determined *via* refractive index measurements by Hristova and White.[16] The calculation results are listed in Table 1.

To calculate $D_B{}'$, we used the method described by Nagle and Tristram-Nagle,[12]

$$D'_{\mathrm{B}} = 2D_{\mathrm{C}} + 2D_{\mathrm{H}} \quad (7)$$

$$D_{\mathrm{C}} = \frac{V_{\mathrm{C}}}{A} \quad (8)$$

$$V_{\mathrm{C}} = V_{\mathrm{L}} - V_{\mathrm{H}} \quad (9)$$

$$n_{\mathrm{w}} = \frac{\frac{A_d}{2} - V_{\mathrm{L}}}{v_{\mathrm{w}}} \quad (10)$$

where D_{C} is the lipid tail group thickness and D_{H} is the lipid head group thickness. V_{C} is the lipid tailgroup volume, V_{H} is the lipid headgroup volume and V_{L} is the total volume of one lipid molecule. A is the lipid cross sectional area, v_{w} is the volume of one water molecule and n_{w} is the number of water molecules per lipid.

One can solve for A and feed into the expression for $D_B{}'$ and get

$$D'_{\mathrm{B}} = \frac{V_{\mathrm{C}} d}{n_{\mathrm{w}} v_{\mathrm{w}} + V_{\mathrm{L}}} + 2D_{\mathrm{H}} \quad (11)$$

Put in values for $D_{\mathrm{H}} = 9$ Å obtained by Büldt *et al.* with neutron diffraction,[20] $V_{\mathrm{H}} = 319$ Å^3 by Sun *et al.* with X-ray diffraction,[21] $V_{\mathrm{L}} = 1303.3$ Å^3 by Tristram-Nagle *et al.*[11] with X-ray neutral flotation measurements, $v_{\mathrm{w}} = 30$ Å^3, n_{w} and d data given by Hristova and White,[16] we get values for $D_B{}'$ and a. These are given in Table 1.

Tristram-Nagle *et al.*[11] also have done detailed studies of DOPC swelling with osmotic pressure and published data of osmotic pressure *vs.* DOPC multilayer water spacing a, and osmotic pressure *vs.* d-spacing.[22] When we compare the results of Tristram-Nagle and Hristova, we found that there is a discrepancy in the number of water molecules per lipid, which leads to a discrepancy in the calculated $D_B{}'$. As listed in Table 1, $D_B{}'$ is between 47.7–48.3 Å, while $D_B{}'$ from ref. 11 is between 45.3–46.5 Å in the same hydration range. This ~2 Å discrepancy in bilayer spacing would lead to a shift of plots of osmotic pressure *vs.* water spacing a for the two published data sources.

However, when plotting the two data sources of osmotic pressure *vs.* d-spacing of DOPC, they agree very well, as shown in Fig. 5. So we decided to combine the two published data of osmotic pressure *vs.* d-spacing, and fit with the function (4) by making $D_B{}'$ a fitting parameter together with A_{fl}, λ_{fl}, A_{h}, λ_{h}, H. The combined data set should give better accuracy than fitting either data alone.

There are multiple sets of parameters which can fit the data equally well if all the parameters are allowed to vary. We have chosen to fix the values of λ_{fl} and A_h at the values obtained by Tristram-Nagle *et al.*[11] Since our purpose is to obtain a calibration curve for the *d*-spacing *vs.* osmotic pressure, we do not concern ourselves with the significance of the actual values of the fitted parameters. The result of the fitting is shown in Fig. 5 and Table 2. The fitted D_B' value is close to ref. 11.

With this calculated standard curve of P_{osm} *vs. d*-spacing, we can convert to RH *vs. d*-spacing using the relation between osmotic pressure and relative humidity[1]

$$P_{osm} = - \left(\frac{kT}{v_w} \right) \ln(\text{RH}). \quad (12)$$

The fitted curve of *d*-spacing *vs.* RH is plotted in Fig. 6 together with the data of Hristova and White[16] and Tristram-Nagle *et al.*[11] Also shown are our measured values of the DOPC *d*-spacing at various values of T. The measured DOPC *d*-spacings *vs.* T are plotted in Fig. 7(a). By putting these measured *d*-spacings onto the standard curve, we can establish the RH *vs.* T plot for our chamber environment (see Fig. 7(b)) which we shall now discuss in the next section.

III. Direct calculation of RH vs. DT using thermodynamic theory

Besides the experimental approach, we can also directly calculate the RH *vs.* T. from thermodynamic theory. This can serve as a reliability check for our experimental calibration.

Assuming ideal behavior, the RH at the reservoir is

$$r_{reservoir} = \frac{P}{P_{H_2O}*} = x_{H_2O}^{vapour} = x_{H_2O}^{liquid} = 1 - \varphi \quad (13)$$

Here, P is the partial pressure of water vapor at the reservoir, $P_{H_2O}*$ is the saturated water vapor pressure, $x_{H_2O}^{vapor}$ is the mole fraction of water in vapor and $x_{H_2O}^{liquid}$ is the mole fraction of water in liquid and φ is the mole fraction of solute in the reservoir.

According to the Clausius–Clapeyron equation for a liquid– gas equilibrium,

$$\frac{d\ln(P)}{dT} \approx \frac{\Delta H_m}{RT^2} \quad (14)$$

where H_m is the enthalpy of vaporization of water and T is the sample temperature which is not near the critical temperature T_c. The equation can be re-written as

$$\ln \left(1 + \frac{\Delta P}{P} \right) \approx \frac{\Delta P}{P} \approx \frac{\Delta H_m \Delta T}{RT^2} \quad (15)$$

where P, T and P are respectively the temperature difference and the difference in partial pressure of water vapor between the sample and the reservoir.

Thus we have

$$r_{\text{sample}} \approx r_{\text{reservoir}} - \frac{\Delta H_{\text{m}} \Delta T}{RT^2} \quad (16)$$

where r_{sample} and $r_{\text{reservoir}}$ are RH at the sample and the reservoir respectively. This shows that to first order, the change in RH is proportional to the change in temperature T. By putting in numbers of $H_{\text{m}} = 40.68$ kJ mol^{-1}, $RT = 25.249$ J mol^{-1} and $T = 304$ K, we obtain $\frac{\Delta H_{\text{m}}}{RT^2} = 0.0530$. Comparing this result to our experimental result in Fig. 7(b), our experimental result also shows a linear relation except for the last 4 points at RH > 0.9995. The linear fit of this data gives a slope of 0.0209, which is less than half of the theory predicted value.

After careful examination of the *d*-spacing equilibration time, we hypothesize that the reason for the last four points falling off the straight in Fig. 7(b) is that we did not allow enough time for the *d*-spacing to equilibrate. The waiting time at each temperature before measurement was around 20–25 min, which is not enough when RH gets very close to 100%.

We also carefully examined the temperature gradient in our chamber, and concluded that the discrepancy in the slope of linear fit is caused by a small temperature gradient between the sponge and the copper top. The temperature sensor for the reservoir is embedded in the copper top for good thermal contact. When heating up the reservoir relative to the sample, the temperature gradient is always negative from the copper to the sponge, which means the sponge is a little cooler than the sensor reading. This leads to a smaller experimental slope than the theoretically predicted value. In conclusion, the temperature differentials plotted are nominal temperature differentials, not the actual temperature between the sample and reservoir. The fact that our data fall onto a linear relation predicted by thermodynamic theory when translated to RH *vs.* d*T* plot provides further support for the RH *vs.* *d*-spacing standard.

Detailed analysis of more lipid multilayer data using this humidity control setup will be presented separately in other papers by Y. Ma *et al.*, (in preparation).

Discussion

I. Comparison with other literature

There are other papers in the literature reporting the evolution of the *d*-spacing of DOPC with RH, such as the paper by Caracciolo *et al.*[15] We make a comparison of our simulations according to Petrache's method, Hristova and White's data, Tristram-Nagle's data with Caracciolo *et al.*'s data for the range of RH very close to 100% (Fig. 6). As can be seen, there is a significant discrepancy in Caracciolo's data compared to the rest. The theory used by Petrache *et al.* from literature predicts a non-linear and diverging behavior of lipid *d*-spacing with change in RH at high RH range, and Hristova and White and Tristram Nagle's data also suggest that, while Caracciolo *et al.*'s data shows an almost linear relation at the same range.

We think that the discrepancy can come from 2 sources. Firstly, Caracciolo *et al.*'s study was time dependent. The measurement of *d*-spacing was done while the humid air was continuously flowing into the chamber and increased RH in real time. At lower humidities, the *d*-spacing changes slowly with RH, so it can still catch up and be close to equilibrium; however, at high RH values close to 1, the *d*-spacing changes are much larger for the same amount of change in RH due to the divergent behavior, and thus in real-time the *d*-spacing no longer catches up with the change of RH therefore the measurements "on the fly" are not under equilibrium conditions. For example, measurements by Servantes[23] show that it can take up to several hours for a multilayer to equilibrate for RH near 100%.

A second possibility is the non-accurate reading from the RH sensor. The humidity is measured with a humidity sensor in Caracciolo *et al.*'s study while Hristova and White's data are PVP weight fraction calculated from refraction index measurements on the sample. It is well known that for the current humidity sensors on the market, the accuracy is around ±1%, and would not be able to determine changes on the order of 0.1% or less. So in this case, it is quite possible that the RH sensor is already saturated when RH is close to 1 and yields readings larger than the actual humidity in the chamber. On the other hand, the refraction index measurements can be more accurate for determining the PVP weight concentration and thus give a more accurate measure when converted to RH.

II. Discussion of errors

To estimate the error of RH, we need the error of *d*-spacing measurements, and also the error in the standard conversion curve. The error bars for the *d*-spacing measurements in Fig. 7(a) are between 0.014 Å to 0.031 Å, which are 0.02–0.05% errors, much smaller than the symbol size to plot. We can estimate the errors of the standard conversion curve from the reduced Chi-square of the fitting. The reduced Chi-square is 0.10 in the $\ln P$ fit, so the dP/P is approximately $\sqrt{0.10} = 0.32$. From the differential of eqn (12), we can get the error of RH between 0.32% to 0.00047% in the RH range 99% to 99.999%.

III. Advantages of the present method

We believe that our compact and economic chamber design together with using a calibration standard would be helpful for future studies of soft materials and bio materials which rely on a high humidity environment. In our own experiments we put a standard DOPC sample with an actual sample side by side. By switching the two in and out of the X-ray beam, one can get the RH value from measuring the *d*-spacing of the DOPC multilayer and also get real measurements from the actual sample under the same conditions. If one is confident about the thermal contact between the sponge and the cell, as well as the accuracy of salt solution, one can also use the calibration curve to control T without using a DOPC sample once the cell is calibrated.

There are three main advantages of this method. Firstly, it is clear that in the multilayer case, compared to measurements in solution with PVP, our results using a vapor chamber have better accuracy (smooth curve) and stronger signal (we can still see the third order diffraction peak at 100% RH). Secondly, our method makes it possible to change the RH of the environment by simply tuning the temperature differential, which enables measurements

under different conditions on the same piece of sample. In the PVP method, one has to make a different sample for each PVP concentration. For experiments with large sample-to-sample variance but looking for subtle changes in a given sample under different conditions (which might be true for a lot of soft matter experiments), this can be a big advantage. Finally, samples under saturated vapor pressure are more amenable to studies using X-rays and neutrons since problems associated with absorption and scattering in the water overlayer are not present.

IV. Further discussion

There are some points to be noted for designing and using such a chamber. First of all, using a non-saturated salt reservoir instead of pure water can help because it lowers the reference RH, at the same time increasing the required temperature differential. Secondly, the extremely compact design of the sample chamber makes a difference. As demonstrated, our chamber is 2.5 inch in outer diameter, which can fit in one's palm. The small volume makes temperature control much easier – less non-uniformity and faster equilibration. The parts are easy to make, assemble, maintain and transport.

It is also worth noting that this chamber design works best at temperatures a few degrees above ambient temperature. With only heating elements, the chamber will not operate below ambient temperature; on the other hand, if the temperature is set too far above from ambient temperature, water condensation on the inner window can create problems and frequent wiping is required. For lower and higher temperatures (such as 10 C and 50 C), an additional temperature regulated layer of enclosure outside our described cell is recommended to raise or lower the ambient temperature.

Last but not least, the chamber can be equipped and used for a wide range of non-contact measurements. For example, our chamber can do X-ray experiments at the same time as optical microscopy. For contact experiments, similar principles apply, one simply has to pay special attention to the sealing of the chamber and avoidance of cold spots.

Acknowledgements

Notes and References

1. Rand RP, Parsegian VA. Biochim. Biophys. Acta, Rev. Biomembr. 1989; 988:351–376.

2. Katsaras J. Biophys. J. 1998; 75:2157–2162. [PubMed: 9788909]

3. Katsaras J, Watson MJ. Rev. Sci. Instrum. 2000; 71:1737–1739.

4. Ku erka N, Liu Y, Chu N, Petrache HI, Tristram-Nagle S, Nagle JF. Biophys. J. 2005; 88:2626–2637. [PubMed: 15665131]

5. Chu N, Ku erka N, Liu Y, Tristram-Nagle S, Nagle JF. Phys. Rev. E: Stat., Nonlinear, Soft Matter Phys. 2005; 71:041904.

6. Tidswell IM, Rabedeau TA, Pershan PS, Kosowsky SD. Phys. Rev. Lett. 1991; 66:2108–2111. [PubMed: 10043393]

7. Alvine KJ, Shpyrko OG, Pershan PS, Shin K, Russell TP. Phys. Rev. Lett. 2006; 97:175503. [PubMed: 17155482]

8. Gang O, Alvine KJ, Fukuto M, Pershan PS, Black CT, Ocko BM. Phys. Rev. Lett. 2005; 95:217801. [PubMed: 16384184]

9. Nagle JF, Katsaras J. Phys. Rev. E: Stat. Phys., Plasmas, Fluids, Relat. Interdiscip. Top. 1999; 59:7018–7024.

10. Li C, Constantin D, Salditt T. J. Phys.: Condens. Matter. 2004; 16:S2439–S2453.

11. Tristram-Nagle S, Petrache HI, Nagle JF. Biophys. J. 1998; 75:917–925. [PubMed: 9675192]

12. Nagle JF, Tristram-Nagle S. Biochim. Biophys. Acta, Rev. Biomembr. 2000; 1469:159–195.

13. Petrache HI, Tristram-Nagle S, Nagle JF. Chem. Phys. Lipids. 1998; 95:83–94. [PubMed: 9807810]

14. Salditt T. J. Phys.: Condens. Matter. 2005; 17:R287–R314.

15. Caracciolo G, Petruccetti M, Caminiti R. Chem. Phys. Lett. 2005; 414:456–460.

16. Hristova K, White SH. Biophys. J. 1998; 74:2419–2433. [PubMed: 9591668]

17. Petrache HI, Gouliaev N, Tristram-Nagle S, Zhang R, Suter RM, Nagle JF. Phys. Rev. E: Stat. Phys., Plasmas, Fluids, Relat. Interdiscip. Top. 1998; 57:7014–7024.

18. Parsegian, V. Van der Waals forces: a handbook for biologists, chemists, engineers, and physicists. Vol. 82. Cambridge University Press; 2005.

19. Vink H. Eur. Polym. J. 1971; 7:1411–1419.

20. Büldt G, Gally HU, Seelig J, Zaccai G. J. Mol. Biol. 1979; 134:673–691. [PubMed: 537074]

21. Sun W-J, Suter RM, Knewtson MA, Worthington CR, Tristram-Nagle S, Zhang R, Nagle JF. Phys. Rev. E: Stat. Phys., Plasmas, Fluids, Relat. Interdiscip. Top. 1994; 49:4665–4676.

22. Petrache HI, Tristram-Nagle S, Gawrisch K, Harries D, Parsegian VA, Nagle JF. Biophys. J. 2004; 86:1574–1586. [PubMed: 14990484]

23. Servantes, ME. Master thesis. Physics, Northern Illinois University; 2011 Dec. A Study of Supported Lipid Multilayers in a Humidity Controlled Environment.
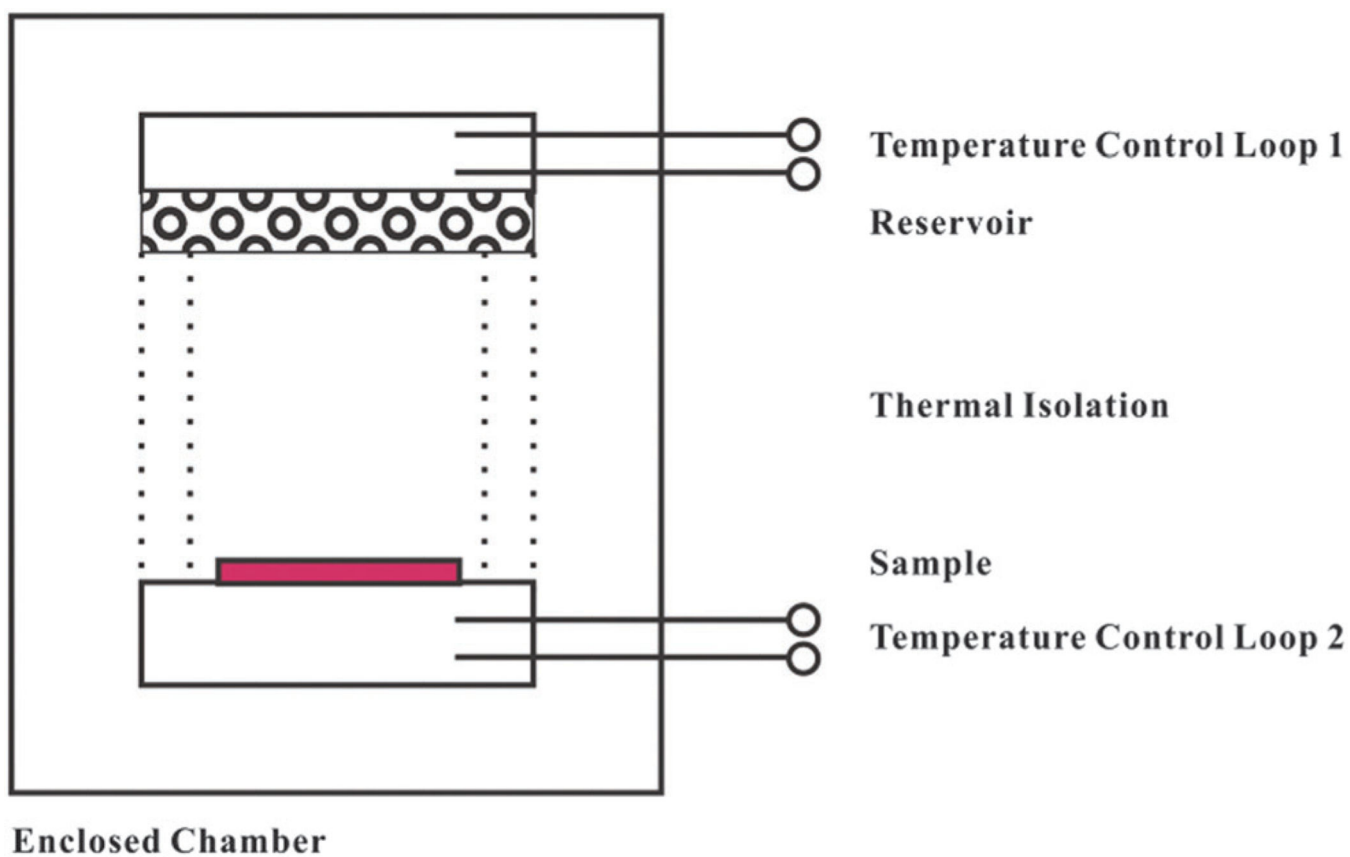
Fig. 1.
Schematic diagram of humidity control design. Inside the enclosed chamber, two independent temperature control loops are set up for the reservoir and the sample. Thermal isolation material is required in between to isolate the two temperature control loops.
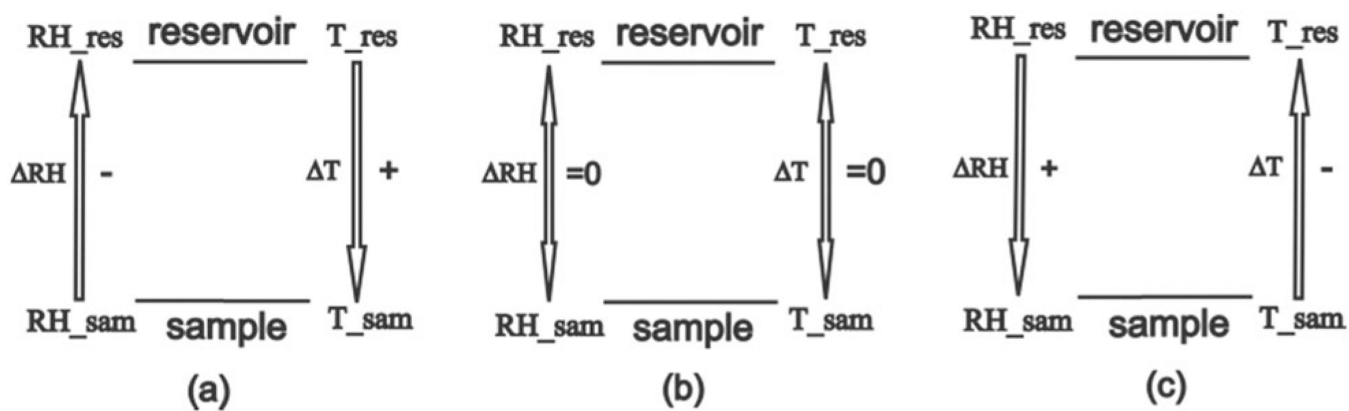
Fig. 2.
Schematics of the principle of temperature differential method applied to relative humidity control. By controlling the temperature differential between the reservoir and the sample (shown as arrows on the right side of each diagram), a relative humidity differential will be generated (shown as arrows on the left of each diagram). As demonstrated by the arrow directions, the relative humidity differential generated is in the opposite direction to the temperature differential.
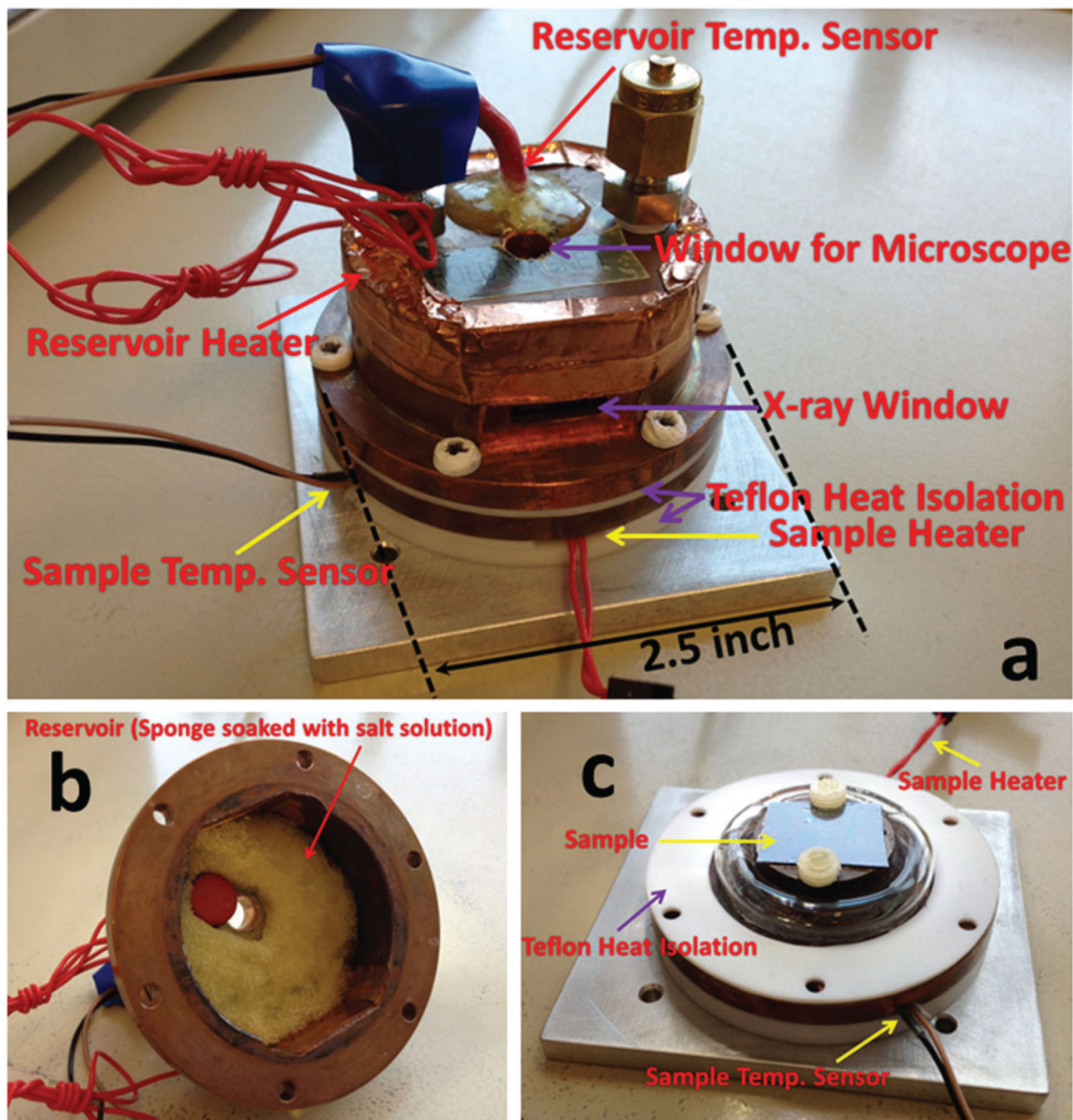
Fig. 3.
Pictures of our RH control chamber for X-ray scattering and optical microscopy measurements. (a) Shows the assembled view, where the arrows mark all the functioning parts. The outer diameter of the chamber is 2.5 inch. The sponge sits inside the top to soak reservoir solution, as shown in opened view (b). The sample mounts on top of the bottom part, as shown in (c).
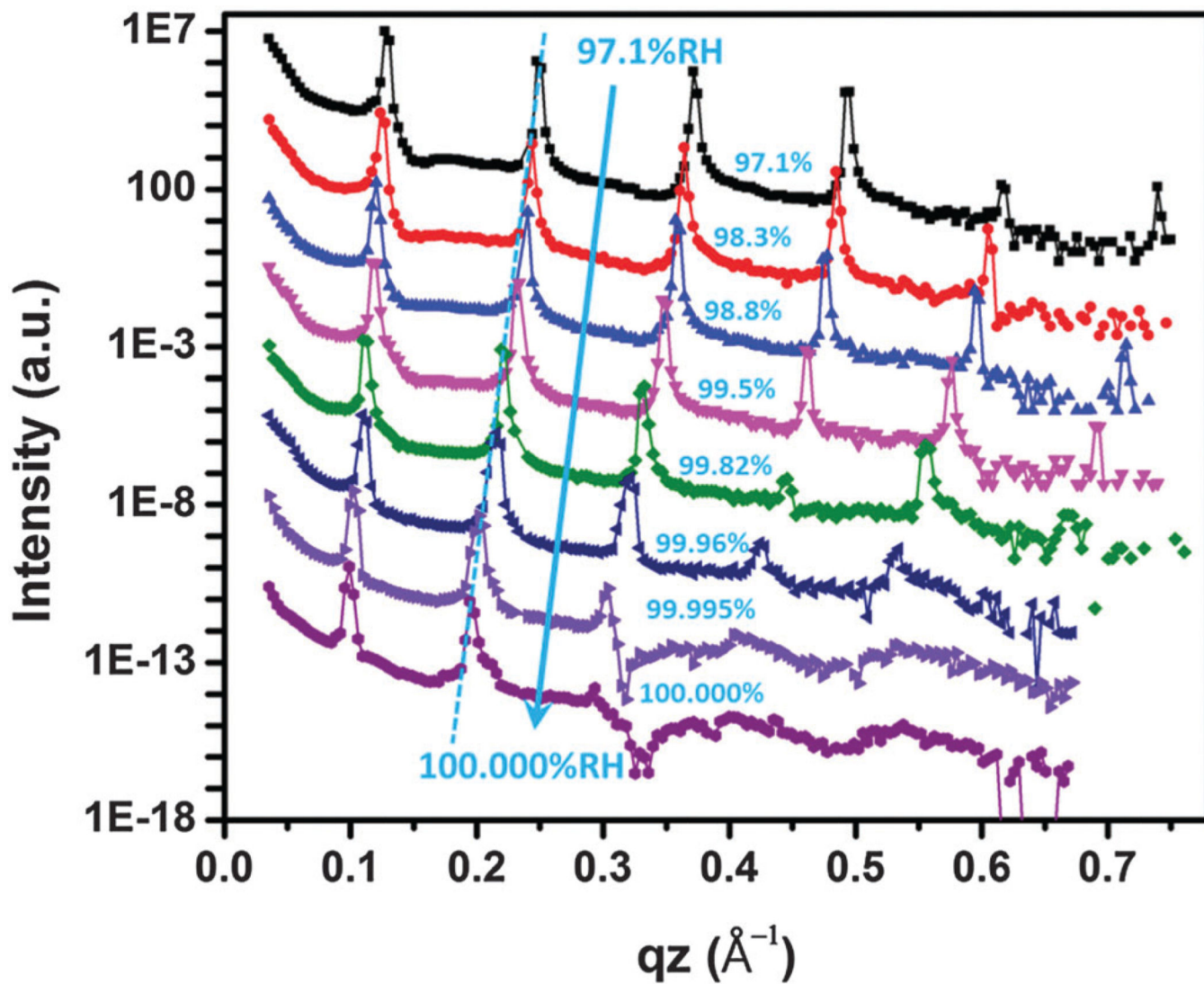
Fig. 4.
X-ray diffraction measurements of a DOPC multilayer sample with different RH. From top to bottom curve, the RH is increased from 97.1% to 100.000%. The RH values corresponding to each curve are indicated to the precision warranted by the percentage accuracy of the calibration. The dashed line marks the peak shifts to lower q_z values with increase of relative humidity.
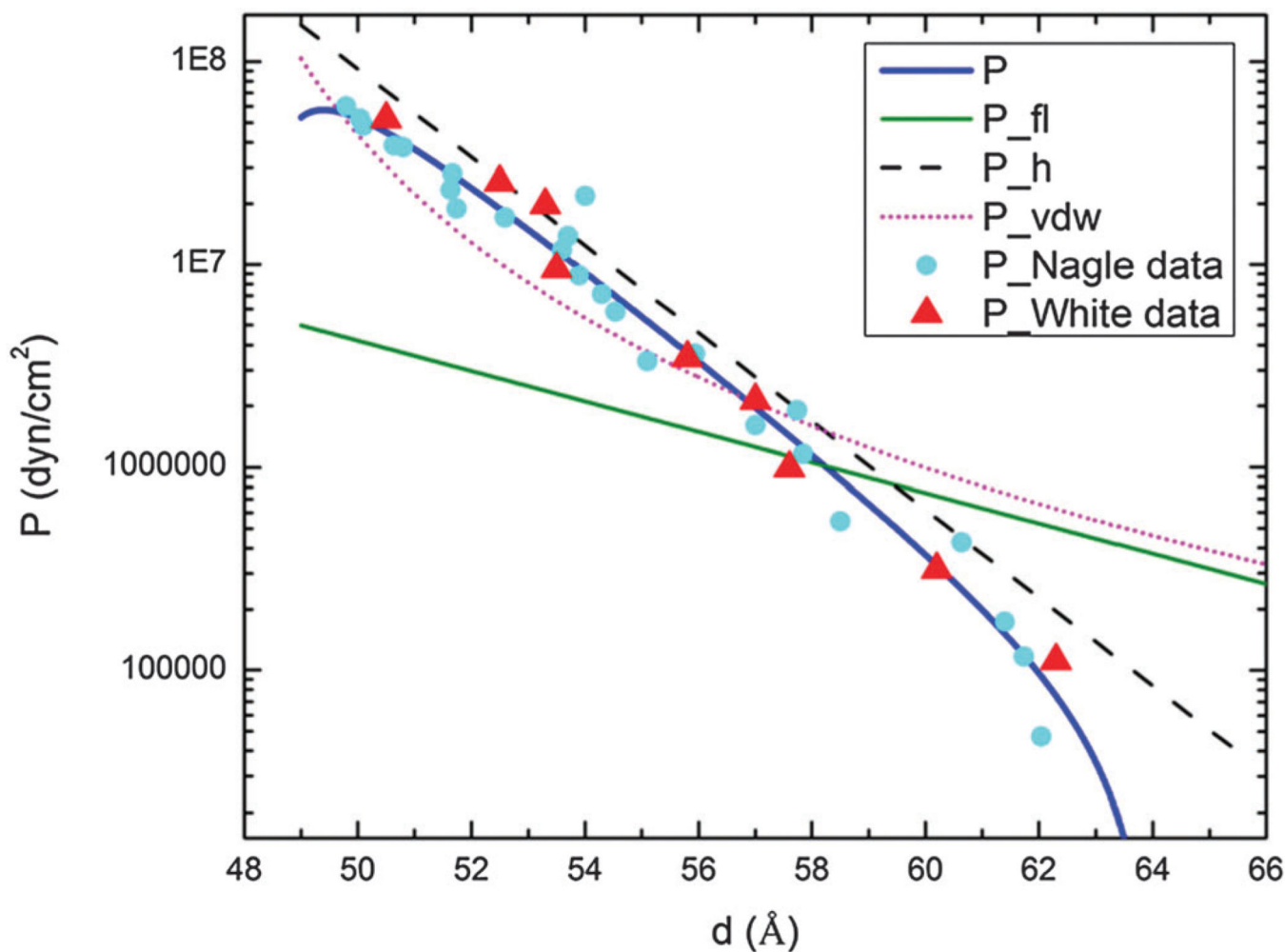
Fig. 5.
Simulation of osmotic pressure *vs. d*-spacing curve fits to Hristova and White's data[16] and Tristram-Nagle's data[11] combined according to method used by Petrache *et al.*[17] The red triangles mark Hristova and White's data, the blue dots mark Tristram-Nagle's data, the curved solid blue line shows the fit to log(osmotic pressure) *vs. d*-spacing. The straight solid green line shows the fluctuation pressure, the straight dashed black line shows the hydration pressure, and the curved dotted pink line shows the van der Waals pressure. Parameter values are given in Table 2.
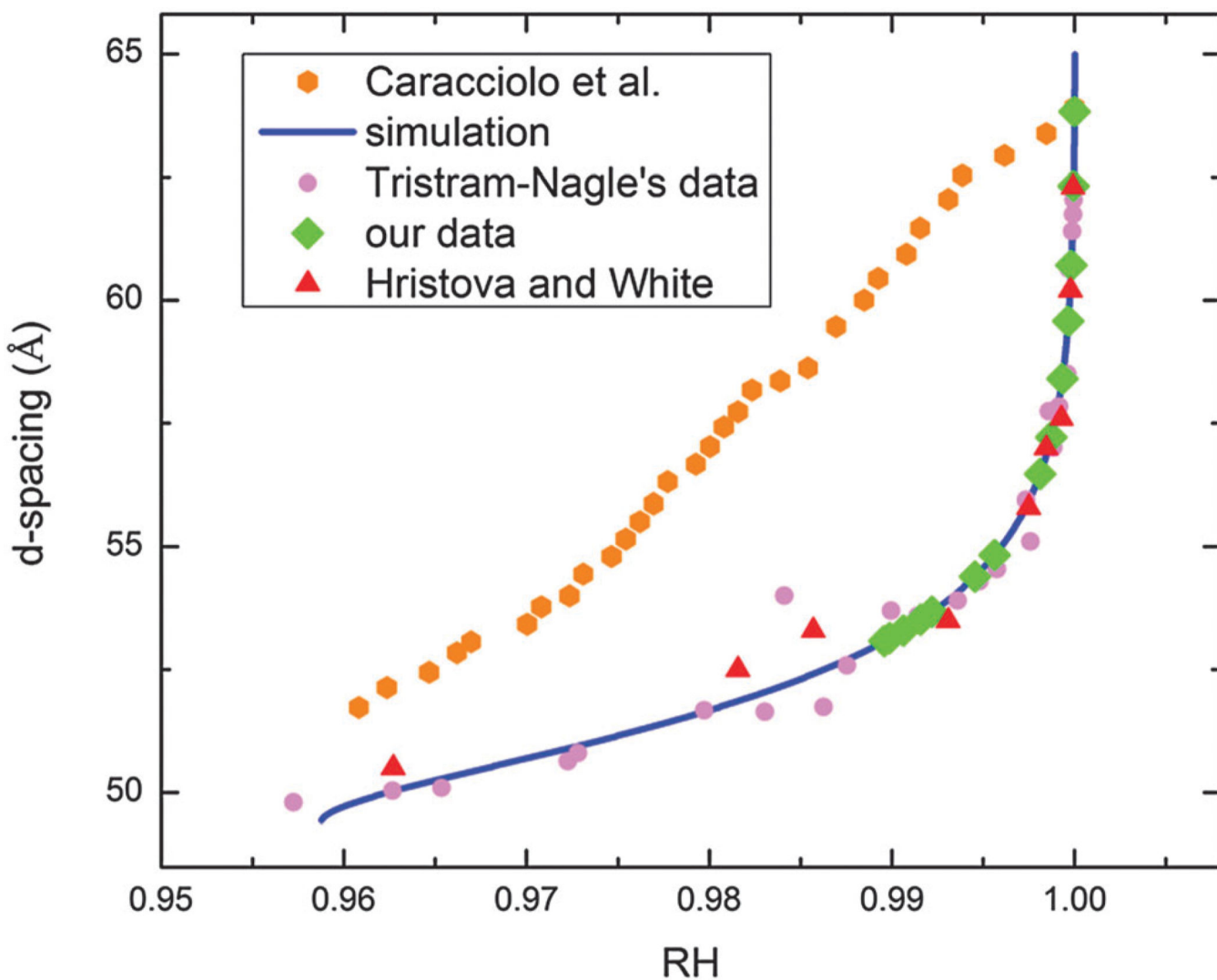
Fig. 6.

Comparison of DOPC *d*-spacing *vs.* humidity plots from different sources. Orange hexagonal are data published by Caracciolo *et al.*[15] Red triangles are the data published by Hristova and White,[16] translated from PVP to RH using the method described in the text. Pink dots are by Tristram-Nagle,[11,22] translated from osmotic pressure to RH. The blue line is our simulation shown in Fig. 5 translated from osmotic pressure to RH with the same method. The green diamonds are our data translated according to the standard curve.
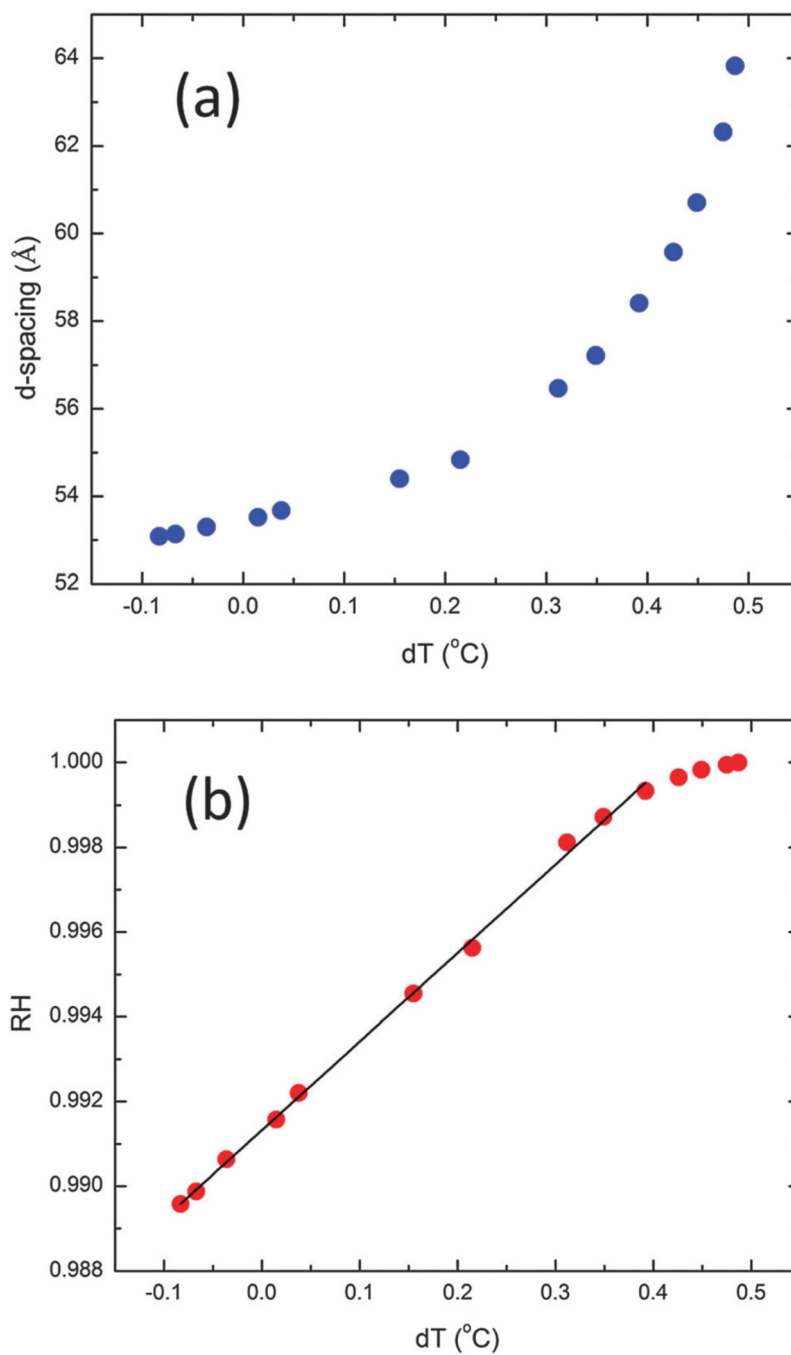
Fig. 7.
Plots of DOPC *d*-spacing (a) and relative humidity (b) *vs.* temperature differential. Relative humidity values in (b) are mapped from DOPC *d*-spacings according to our simulation as shown with blue line in Fig. 6. The temperature differentials plotted are nominal values, since we were not able to directly measure the temperature at the sponge.

Table 1

Calculated values for D_B' and a according to Hristova and White's data[16]

PVP (%)	ln P (dyn cm^{-2})	D_B' (Å)	a (Å)	d (Å)
58.54	17.7682	48.0	2.5	50.5
46.71	17.0538	48.2	4.3	52.5
42.97	16.7977	48.3	5.0	53.3
33.63	16.0689	47.6	5.9	53.5
23.42	15.0553	47.7	8.1	55.8
19.53	14.5723	47.8	9.2	57.0
14.39	13.8049	47.3	10.3	57.6
8.69	12.6616	47.5	12.7	60.2
5.09	11.6200	47.4	14.9	62.3

Table 2

Parameter values for the fit to ln P data. The parameters in bold are the ones being varied

A_{fl} (10^6 dyn cm^{-2})	λ_{fl} (Å)	A_h (10^9 dyn cm^{-2})	λ_h (Å)	H (10^{-14} erg)	D_B' (Å)
8.37	5.8	0.68	**2.0**	**5.28**	**46.0**